Applied Catalysis B: Environmental 147 (2014) 387–393

Contents lists available at ScienceDirect

Applied Catalysis B: Environmental

journal homepage: www.elsevier.com/locate/apcatb

Palladium(0) nanoparticles supported on silica-coated cobalt ferrite: A highly active, magnetically isolable and reusable catalyst for hydrolytic dehydrogenation of ammonia borane

Serdar Akbayrak[a], Murat Kaya[b,*], Mürvet Volkan[a], Saim Özkar[a]

[a] Department of Chemistry, Middle East Technical University, 06800 Ankara, Turkey
[b] Department of Chemical Engineering and Applied Chemistry, Atilim University, 06836 Ankara, Turkey

ARTICLE INFO

Article history:
Received 18 July 2013
Received in revised form
11 September 2013
Accepted 16 September 2013
Available online 26 September 2013

Keywords:
Palladium nanoparticles
Silica coated
Magnetic cobalt ferrite
Ammonia borane
Dehydrogenation

ABSTRACT

Palladium(0) nanoparticles supported on silica-coated cobalt ferrite ($Pd(0)/SiO_2–CoFe_2O_4$) were in situ generated during the hydrolysis of ammonia borane, isolated from the reaction solution by using a permanent magnet and characterized by ICP-OES, XRD, TEM, TEM-EDX, XPS and the N_2 adsorption–desorption techniques. All the results reveal that well dispersed palladium(0) nanoparticles were successfully supported on silica coated cobalt ferrite and the resulting $Pd(0)/SiO_2–CoFe_2O_4$ are highly active, magnetically isolable, and recyclable catalysts in hydrogen generation from the hydrolysis of ammonia borane with an unprecedented turnover frequency (TOF, calculated on the basis of the total amount of Pd) of 254 mol H_2 (mol Pd min)$^{-1}$ at 25 ± 0.1 °C. The reusability tests reveal that $Pd(0)/SiO_2–CoFe_2O_4$ are still active in the subsequent runs of hydrolysis of ammonia borane providing 100% conversion. $Pd(0)/SiO_2–CoFe_2O_4$ provide the highest catalytic activity with a TOF value of 198 mol H_2 (mol Pd min)$^{-1}$ in the 10th use in hydrogen generation from the hydrolysis of ammonia borane as compared to the other palladium catalysts. The work reported here also includes the kinetic studies depending on the temperature to determine the activation energy of the reaction ($E_a = 52 \pm 2$ kJ/mol) and the effect of catalyst concentration on the rate of hydrolytic dehydrogenation of ammonia borane, respectively.

1. Introduction

Hydrogen has attracted great interest as a globally accepted clean energy carrier [1]. Secure storage and effective release of hydrogen are the limiting factors in the application of hydrogen energy [2]. Since there is a big challenge in storing hydrogen securely, much attention has been paid to the solid hydrogen storage materials such as metal hydrides [3] and sorbent materials [4]. Ammonia borane (AB) appears to be the most promising solid hydrogen carrier for on-board applications due to its high hydrogen content (19.6 wt%), high stability under ambient conditions, and nontoxicity [5,6]. More importantly, ammonia borane is able to release its hydrogen upon hydrolysis in the presence of a suitable catalyst (Eq. (1)).

$$H_3NBH_3(aq) + 3\ H_2O(l) \xrightarrow{\text{catalyst}} NH_4BO_2(aq) + 3\ H_2(g) \quad (1)$$

Many transition metal nanoparticles have been tested as catalyst in the hydrolytic dehydrogenation of AB [7]. However, most of the transition metal nanoparticles suffer in long-term stability because of the aggregation into clumps and ultimately to the bulk metal which would cause a significant loss in catalytic activity [8,9]. Therefore they must be stabilized against aggregation into larger particles [10]. Graphenes [11,12], carbon nanotubes [13,14], carbon black [15], zeolites [16,17], alumina [18,19], hydroxyapatites [20] and polymers [21] have been widely used as supporting materials in the preparation of metal nanoparticles with controllable size and size distribution. Although the use of carbonaceous supporting materials, providing well dispersion of metal nanoparticles with high external surface area [22], seems to be favorable in comparison with metal oxides or polymers, the separation of such catalysts from the reaction medium is difficult during the filtration and centrifugation process. The use of porous oxides as stabilizing agent is also limited because metal nanoparticles can easily migrate and block the entrance of pores after several uses. Therefore, magnetically recoverable catalysts have attracted great interest in liquid phase reactions due to their easy magnetic separation making the recovery of catalysts much easier than by filtration or centrifugation [23].

Herein, we report palladium(0) nanoparticles supported on silica-coated cobalt ferrite ($SiO_2–CoFe_2O_4$) as magnetically isolable and recyclable catalyst in hydrogen generation from the hydrolysis

* Corresponding author. Tel.: +903125868304; fax: +903125868091.
E-mail address: mmuratkaya@gmail.com (M. Kaya).

0926-3373/$ – see front matter © 2013 Elsevier B.V. All rights reserved.
http://dx.doi.org/10.1016/j.apcatb.2013.09.023

of ammonia borane. Palladium(II) ions were impregnated on silica-coated cobalt ferrite from the aqueous solution of palladium(II) nitrate and then reduced by ammonia borane forming the palladium(0) nanoparticles supported on silica-coated cobalt ferrite, ($Pd(0)/SiO_2–CoFe_2O_4$), which were isolated from the reaction solution by using a permanent magnet and characterized by ICP-OES, XRD, TEM, TEM-EDX, XPS and the N_2 adsorption–desorption techniques. All the results reveal that highly dispersed palladium(0) nanoparticles were successfully supported on $SiO_2–CoFe_2O_4$. $Pd(0)/SiO_2–CoFe_2O_4$ are highly active and recyclable catalysts in hydrogen generation from the hydrolysis of ammonia borane with an unprecedented turnover frequency of 254 min^{-1} at 25 ± 0.1 °C.

2. Experimental section

2.1. Materials

Iron(III) chloride ($FeCl_3$), tetraethylorthosilicate (TEOS), ammonium hydroxide (NH_4OH), sodium hydroxide (NaOH), cobalt(II) chloride ($CoCl_2$), palladium(II) nitrate ($Pd(NO_3)_2{\cdot}xH_2O$), and ammonia borane (H_3NBH_3, 97%) were purchased from Aldrich. Deionized water was distilled by water purification system (Milli-Q System). All glassware and Teflon-coated magnetic stir bars were cleaned with acetone, followed by copious rinsing with distilled water before drying in an oven at 150 °C.

2.2. Characterization

Palladium content of the $Pd(0)/SiO_2–CoFe_2O_4$ samples were determined by Inductively Coupled Plasma Optical Emission Spectroscopy (ICP-OES, Leeman-Direct Reading Echelle). Transmission electron microscopy (TEM) was performed on a JEM-2100F (JEOL) microscope operating at 200 kV. A small amount of powder sample was placed on a copper grid of the transmission electron microscope. Samples were examined at magnification between 100 K and 400 K. The X-ray photoelectron spectroscopy (XPS) analysis was performed on a Physical Electronics 5800 spectrometer equipped with a hemispherical analyzer and using monochromatic Al $K\alpha$ radiation of 1486.6 eV, the X-ray tube working at 15 kV, 350 W and pass energy of 23.5 keV. ^{11}B NMR spectra were recorded on a Bruker Avance DPX 400 with an operating frequency of 128.15 MHz for ^{11}B.

2.3. Preparation of magnetic silica-coated cobalt ferrite ($SiO_2–CoFe_2O_4$)

The preparation of magnetic cobalt ferrite nanoparticles was carried out by modification of previously established procedure [24]. The detailed information on the preparation and characterization of silica-coated cobalt ferrite can be found elsewhere [25]. In a typical experiment 25 mL of 0.4 M iron(III) chloride and 25 mL of 0.2 M of cobalt(II) chloride solutions were mixed at room temperature. Then, in a separate vessel 25 mL of 3.0 M sodium hydroxide solution was prepared and slowly added to the salt solution. After complete addition of NaOH solution, a black suspension was obtained. The mechanical stirring was continued for 1 h at 80 °C. Then the solution was cooled to room temperature and the black precipitates were collected by using an external magnet. The supernatant was removed and the particles were washed three times with deionized water–ethanol solution and then the particles were dispersed in 50 mL of water. Silica coating was applied by using a modified version of Stöber method [26]. For that, 200 mL ethanol, 1 mL TEOS and 0.5 mL of NH_4OH were added to the reaction mixture and subsequently 50 mL cobalt ferrite colloid was added to the mixture and stirred for 4 h at room temperature. After the formation of the thick silica shell, particles were collected with a magnet and washed three times with deionized water. The resulting silica coated cobalt ferrite nanoparticles ($SiO_2–CoFe_2O_4$) were separated by using a permanent magnet and washed with excess ethanol and dried at 120 °C for 12 h in the oven.

2.4. Impregnation of palladium(II) ions on magnetic silica-coated cobalt ferrite [$Pd(0)/SiO_2–CoFe_2O_4$]

$SiO_2–CoFe_2O_4$ (100 mg) was added to a solution of $Pd(NO_3)_2{\cdot}xH_2O$ (5.65 mg) in 20 mL H_2O in a 50 mL beaker. This slurry was stirred at room temperature for 12 h and then, the solid particles were isolated from the supernatant solution by using a permanent magnet. Next, the resulting particles $Pd(II)/SiO_2–CoFe_2O_4$ were washed with 20 mL of deionized water and isolated by using a permanent magnet and dried at 120 °C for 12 h in the oven.

2.5. In situ formation of palladium(0) nanoparticles supported on magnetic silica-coated cobalt ferrite [$Pd(0)/SiO_2–CoFe_2O_4$] and concomitant catalytic hydrolysis of AB

Palladium(0) nanoparticles supported on magnetic silica-coated cobalt ferrite were in situ generated from the reduction of $Pd(II)/SiO_2–CoFe_2O_4$ during the catalytic hydrolysis of AB. Before starting the catalyst formation and concomitant catalytic hydrolysis of AB, a jacketed reaction flask (20 mL) containing a Teflon-coated stir bar was placed on a magnetic stirrer (Heidolph MR-301) and thermostated to 25.0 ± 0.1 °C by circulating water through its jacket from a constant temperature bath. Then, a graduated glass tube (60 cm in height and 3.0 cm in diameter) filled with water was connected to the reaction flask to measure the volume of the hydrogen gas to be evolved from the reaction. Next, 10 mg powder of [$Pd(II)/SiO_2–CoFe_2O_4$] (1.98 wt% Pd) was dispersed in 10 mL distilled water in the reaction flask thermostated at 25.0 ± 0.1 °C. Then, 31.8 mg AB (1.0 mmol $H_3N\,BH_3$) was added into the flask and the reaction medium was stirred at 1000 rpm. After adding ammonia borane, palladium(0) nanoparticles were formed and the catalytic hydrolysis of AB started immediately. The volume of hydrogen gas evolved was measured by recording the displacement of water level every 30 s at constant atmospheric pressure of 693 Torr. The reaction was stopped when no more hydrogen evolution was observed. In each experiment, the resulting solutions were filtered and the filtrates were analyzed by ^{11}B NMR and conversion of AB to metaborate anion was confirmed by comparing the intensity of signals in the ^{11}B NMR spectra of the filtrates (see Fig. S1).

2.6. Determination of activation energy for hydrolytic dehydrogenation of AB catalyzed by [$Pd(0)/SiO_2–CoFe_2O_4$]

In a typical experiment, the hydrolysis reaction was performed starting with 10 mL of 100 mM (31.8 mg) AB solution and 10 mg [$Pd(II)/SiO_2–CoFe_2O_4$] (1.98 wt% palladium, [Pd] = 0.186 mM) at various temperatures (20 °C, 25 °C, 30 °C, 35 °C) in order to obtain the activation energy.

2.7. Reusability of $Pd(0)/SiO_2–CoFe_2O_4$ in the hydrolytic dehydrogenation of AB

After the complete hydrolysis of AB started with 10 mL of 100 mM AB (31.8 mg H_3NBH_3), and 40 mg $Pd(0)/SiO_2–CoFe_2O_4$ (1.98 wt% palladium, [Pd] = 0.744 mM) at 25 ± 0.1 °C, the catalyst was isolated using a permanent magnet. $Pd(0)/SiO_2–CoFe_2O_4$ were magnetically attracted to the bottom of the reaction vessel by a magnet, and the upper solution was removed and the catalyst was washed with 10 mL of water before every run in the reusability test.

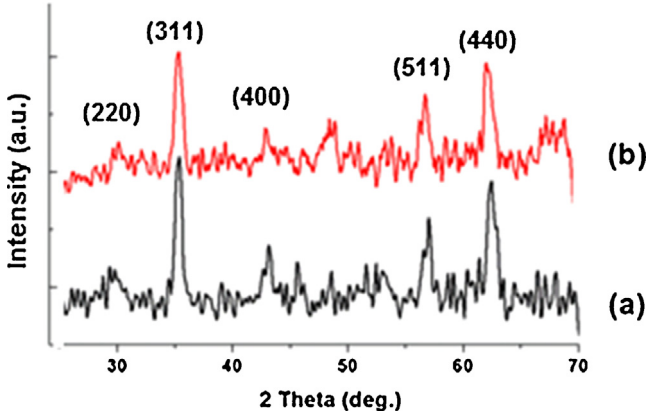

Fig. 1. Powder XRD patterns of (a) SiO_2–$CoFe_2O_4$, (b) Pd(0)/SiO_2–$CoFe_2O_4$ with a 1.98 wt% Pd loading.

After washing, the catalyst was isolated again and the isolated sample of Pd(0)/SiO_2–$CoFe_2O_4$ redispersed in 10 mL solution of 100 mM AB for a subsequent run of hydrolysis at 25 ± 0.1 °C.

3. Results and discussion

Cobalt ferrite ($CoFe_2O_4$) nanoparticles were preferred as magnetic core materials due to the easy preparation procedure [24]. Unlike magnetite (Fe_3O_4), there is no need to use inert atmosphere or organic additives to produce $CoFe_2O_4$ nanoparticles [27–29]. As-prepared nanoparticles are severely agglomerated with poor control of size and shape in most cases, which greatly restrict their applications [29,30]. Thus SiO_2 was used to protect the magnetic core material against leaching and agglomeration while providing high surface area to stabilize the palladium nanoparticles.

Palladium(0) nanoparticles supported on magnetic silica-coated cobalt ferrite were in situ generated during the hydrolytic dehydrogenation of ammonia borane. Palladium(II) ions were impregnated on SiO_2–$CoFe_2O_4$ from the aqueous solution of palladium(II) nitrate and then reduced by AB at room temperature. When AB solution is added to the suspension of SiO_2–$CoFe_2O_4$ containing palladium(II) ions, both reduction of palladium(II) to palladium(0) and hydrogen release from the hydrolysis of AB occur concomitantly. The progress of hydrolytic dehydrogenation of ammonia borane was followed by monitoring the change in H_2 pressure which was then converted into the equivalent H_2 per mole of AB, using the known 3:1 H_2/AB stoichiometry (Eq. (1)). Palladium(0) nanoparticles supported on magnetic silica-coated cobalt ferrite, hereafter referred to as Pd(0)/SiO_2–$CoFe_2O_4$, in situ formed during the hydrolysis of AB, could be isolated from the reaction solution as powder by using a permanent magnet and characterized by ICP-OES, XRD, TEM, TEM-EDX, XPS and the N_2 adsorption–desorption techniques. Palladium content of Pd(0)/SiO_2–$CoFe_2O_4$ was determined by ICP-OES. The comparison of the XRD patterns of SiO_2–$CoFe_2O_4$ and Pd(0)/SiO_2–$CoFe_2O_4$ with a palladium loading of 1.98 wt% Pd, given in Fig. 1a and b, respectively, clearly shows that there is no change in the characteristic diffraction peaks of silica-coated cobalt ferrite. Powder XRD pattern of Pd(0)/SiO_2–$CoFe_2O_4$ in Fig. 1b gives peaks at 30.3°, 35.8°, 43.3°, 57.4° and 62.5° assigned to the (2 2 0), (3 1 1), (4 0 0), (5 1 1) and (4 4 0) reflections of SiO_2–$CoFe_2O_4$, respectively (PDF Card 22-1086). This observation indicates that the host material remains intact after impregnation of palladium(II) ions and their reduction to palladium(0) on the support without noticeable alteration in the framework lattice or loss in the crystallinity and there is no observable peak attributable to palladium nanoparticles in Fig. 1b, probably as a result of low palladium loading of silica-coated cobalt ferrite.

The BET nitrogen adsorption analysis gave the surface area of SiO_2–$CoFe_2O$ and Pd(0)/SiO_2–$CoFe_2O_4$ as 178.72 m^2/g and 171.28 m^2/g, respectively. This slight decrease in the surface area of silica coated cobalt ferrite upon palladium loading implies the existence of palladium(0) nanoparticles on the surface.

Fig. 2 shows the TEM images of silica coated cobalt ferrite and Pd(0)/SiO_2–$CoFe_2O_4$ with a palladium loading of 1.98 wt% taken with different magnifications and the TEM-EDX spectrum taken from the lattice fringes (0.48 nm) of SiO_2–$CoFe_2O_4$ in Fig. 2d, which indicate that: (i) the size of SiO_2–$CoFe_2O_4$ nanoparticles used as support is about 13.0 ± 2.0 nm (Fig. 2a and b) and the size of the palladium(0) nanoparticles are about 6.0 ± 1.0 nm (Fig. 2c and d), (ii) highly dispersed palladium nanoparticles are formed also in the lattice fringes of silica coated cobalt ferrite (Fig. 2d) as seen from the comparison of Fig. 2b and d, the images taken from the area indicated with an arrow in Fig. 2a and c, respectively, (iii) impregnation of palladium(II) followed by reduction to palladium(0) causes no change in the framework lattice of the silica coated cobalt ferrite in agreement with the XRD results, (iv) TEM-EDX spectrum of Pd(0)/SiO_2–$CoFe_2O_4$ with a palladium loading of 1.98 wt% indicating that palladium is the only element detected in the sample in addition to the framework elements of silica coated cobalt ferrite (Si, O, Co, Fe) (Fig. 2e).

The composition of Pd(0)/SiO_2–$CoFe_2O_4$ in situ formed during the hydrolysis of AB and the oxidation state of palladium were also studied by XPS technique. The survey-scan XPS spectrum of Pd(0)/SiO_2–$CoFe_2O_4$ with a palladium loading of 1.98 wt% given in Fig. 3a shows all the framework elements of palladium(0) nanoparticles supported on silica-coated cobalt ferrite in agreement with the TEM-EDX result. High resolution X-ray photoelectron spectrum of a Pd(0)/SiO_2–$CoFe_2O_4$ sample given in Fig. 3b shows two prominent bands at 340.30 eV and 334.9 eV which can readily be assigned to Pd(0) $3d_{3/2}$ and $3d_{5/2}$ bands [31], respectively.

The magnetic property of uncoated $CoFe_2O_4$ nanoparticles and Pd(0)/SiO_2–$CoFe_2O_4$ catalyst were characterized by using the vibrating sample magnetometer (VSM). The hysteresis curves for Pd(0)/SiO_2–$CoFe_2O_4$ catalyst recorded at 300 K are given in Fig. 4. The measured saturation magnetization (M_s) values of the $CoFe_2O_4$ and Pd(0)/SiO_2–$CoFe_2O_4$ particles were 34.7 emu/g and 31.5 emu/g, respectively. Thus, these two materials have similar magnetic properties; only a slight decrease in the saturation magnetization values was observed for the Pd(0)/SiO_2–$CoFe_2O_4$ particles compared to the uncoated ones due to the presence of 3–5 nm nonmagnetic silica shell.

3.1. Catalytic activity of Pd(0)/SiO_2–$CoFe_2O_4$ in the hydrolytic dehydrogenation of AB

Before starting with the investigation on the catalytic activity of Pd(0)/SiO_2–$CoFe_2O_4$ in the hydrolytic dehydrogenation of AB, a control experiment was performed to check whether SiO_2–$CoFe_2O_4$ shows any catalytic activity in the hydrolysis of AB at the same temperature. In a control experiment starting with 1.0 mmol of AB and 10 mg of powder of SiO_2–$CoFe_2O_4$ (the same amount as the one used in catalytic activity tests) in 10 mL of water at 25.0 ± 0.1 °C or 40.0 ± 0.1 °C, no hydrogen generation was observed in 1 h at both temperatures. This observation indicates that the hydrolysis of AB does not occur in the presence of SiO_2–$CoFe_2O_4$ in the temperature range used in this study. However, Pd(0)/SiO_2–$CoFe_2O_4$ are found to be highly active catalyst in the hydrolysis of ammonia borane generating 3.0 equivalent H_2 gas per mol of AB in the same temperature range.

The catalytic activity of Pd(0)/SiO_2–$CoFe_2O_4$ was studied depending on the palladium loading. A series of experiments were performed starting with 10 mL solution of 100 mM AB and 0.186 mM Pd using Pd(0)/SiO_2–$CoFe_2O_4$ sample with various

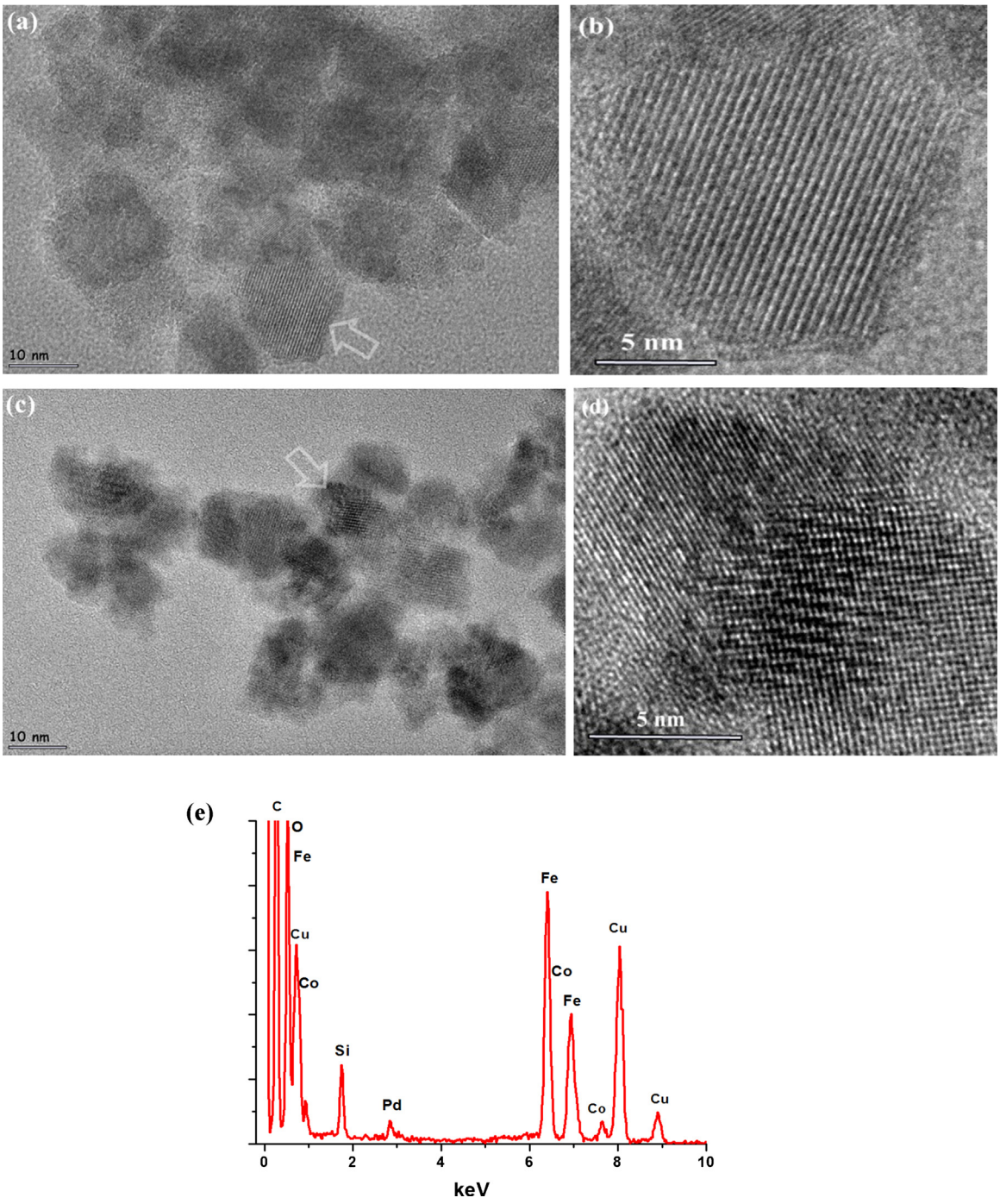

Fig. 2. TEM images of silica coated cobalt ferrite with the scale bar of (a) 10 nm, (b) 5 nm and TEM images of Pd(0)/SiO_2–$CoFe_2O_4$ with a palladium loading of 1.98 wt% with the scale bar of (c) 10 nm, (d) 5 nm, (e) TEM-EDX spectrum of Pd(0)/SiO_2–$CoFe_2O_4$.

palladium loading (0.92 wt%, 1.98 wt%, 2.89 wt%, 3.86 wt%, 4.52 wt% Pd) in appropriate amount to provide the same palladium concentration in all of the experiments. The Pd(0)/SiO_2–$CoFe_2O_4$ sample with palladium loading of 1.98 wt% Pd provides the highest catalytic activity in hydrogen generation from the hydrolysis of AB at 25.0 ± 0.1 °C (Fig. S2). Therefore, Pd(0)/SiO_2–$CoFe_2O_4$.catalyst with palladium loading of 1.98 wt% Pd was used in all of the further experiments performed in this study.

Fig. 5a shows the plots of equivalent H_2 gas generated per mole of H_3NBH_3 versus time during the catalytic hydrolysis of 100 mM AB solution using Pd(0)/SiO_2–$CoFe_2O_4$ with a loading of 1.98 wt% Pd in different catalyst concentration at 25.0 ± 0.1 °C. The hydrogen generation rate was determined from the linear portion of each plot in Fig. 5a and plotted versus the initial concentration of palladium, both in logarithmic scale, in Fig. 5b, which gives straight line with a slope of 0.61 indicating that order of the catalytic hydrolysis of AB with respect to the palladium concentration is 0.61. The TOF value for hydrogen generation from the hydrolysis of AB (100 mM) at 25.0 ± 0.1 °C was determined from the hydrogen generation rate in the linear portion of plots given in Fig. 5a for experiments starting with 100 mM AB plus Pd(0)/SiO_2–$CoFe_2O_4$ with a loading of 1.98 wt% Pd [0.093 mM]. The TOF value of Pd(0)/SiO_2–$CoFe_2O_4$ catalyst is as high as 254 (mol H_2/mol Pd min) in the hydrolytic dehydrogenation of ammonia borane at 25.0 ± 0.1 °C. However, TOF

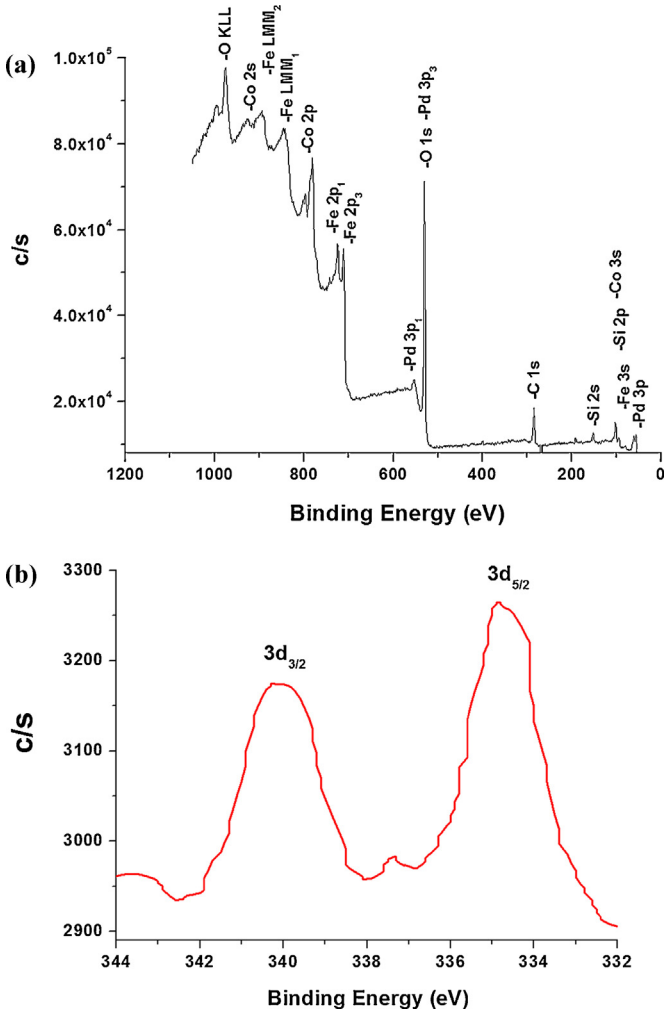

Fig. 3. (a) X-ray photoelectron (XPS) spectrum of Pd(0)/SiO_2–$CoFe_2O_4$ with a palladium loading of 1.98 wt% (b) The high resolution scan of Pd 3d bands.

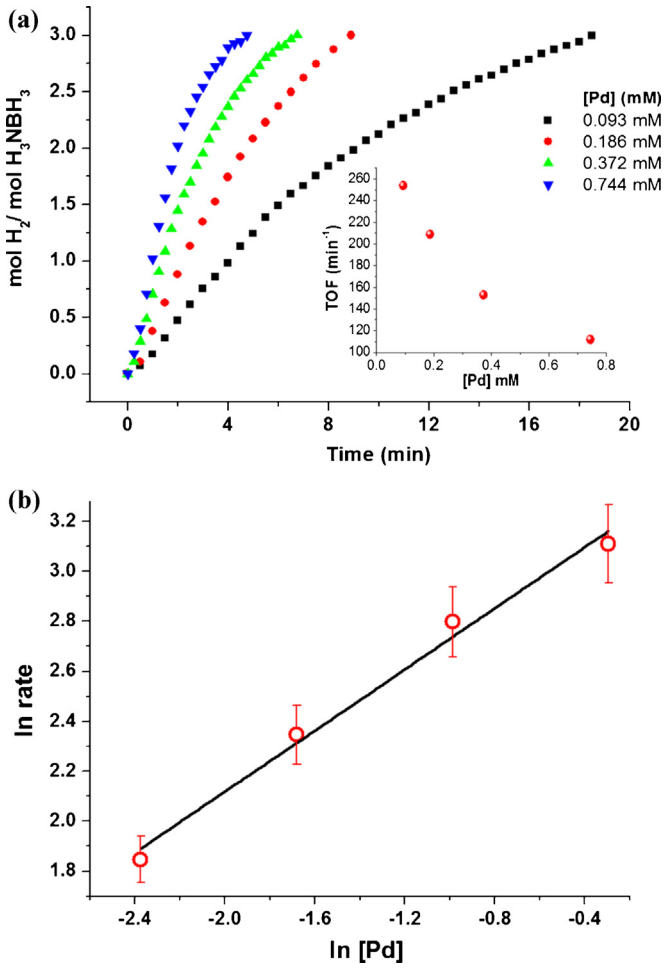

Fig. 5. (a) mol H_2/mol H_3NBH_3 versus time graph depending on the palladium concentration in Pd(0)/SiO_2–$CoFe_2O_4$ for the hydrolytic dehydrogenation of AB (100 mM) at 25.0 ± 0.1 °C. The inset shows the TOF values of the catalyst at different Pd concentrations (b) The logarithmic plot of hydrogen generation rate versus the concentration of Pd; ln (rate) = 0.61 ln [Pd] + 3.34.

value decreases with the increasing palladium concentration as shown in the inset of Fig. 5a. The inverse relation is most likely due to the increasing size of palladium(0) nanoparticles.

In order to compare the catalytic activities of Pd(0)/SiO_2–$CoFe_2O_4$ and Pd(0)/SiO_2, the latter one was prepared by reducing the palladium(II) ions impregnated on a commercial silica (10 nm in size). In a control experiment, 1.0 mmol of AB and an appropriate amount of powder Pd(II)/SiO_2 to provide the same palladium concentration in 10 mL of water were used at 25.0 ± 0.1 °C. The TOF value of Pd(0)/SiO_2 was found as 10 (mol H_2/mol Pd min). Thus, the catalytic activity of Pd(0)/SiO_2 is much less than that of Pd(0)/SiO_2–$CoFe_2O_4$, by a factor of 25.

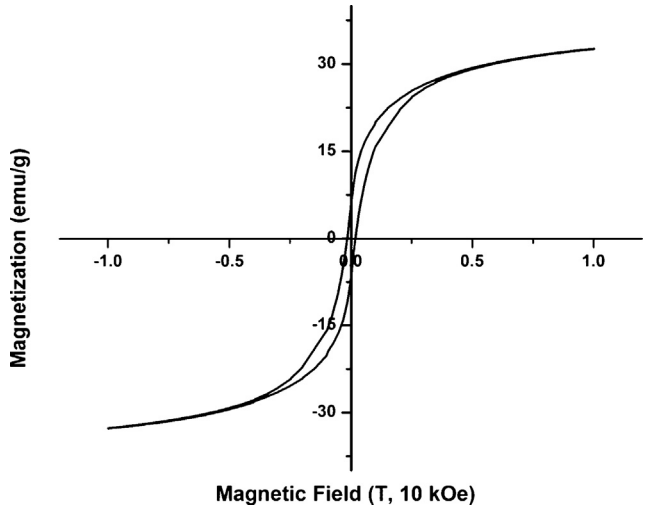

Fig. 4. Field-dependent magnetization curve for SCF measured at 300 K.

TOF values of the reported palladium catalysts used in hydrolytic dehydrogenation of ammonia borane are listed in Table 1 for comparison. As clearly seen from the comparison of values listed in Table 1, Pd(0)/SiO_2–$CoFe_2O_4$ provide the highest TOF value ever reported for the hydrolytic dehydrogenation of AB using palladium catalysts such as Pd@Co/graphene, $Co_{35}Pd_{65}$/C annealed, 2.1 wt% RGO@Pd, $Co_{35}Pd_{65}$/C, CDG-Pd, Pd(0)-HAP, Pd/zeolite, RGO/Pd, PSSA-co-MA-Pd, Pd/γ-Al_2O_3, Pd black.

Activation energy for the hydrolytic dehydrogenation of ammonia borane catalyzed by Pd(0)/SiO_2–$CoFe_2O_4$ was determined from the slope of Arrhenius plot, ln k versus $1/T$ (K^{-1}). The rate constant for the hydrogen generation reactions were calculated from the slope of the linear part of hydrogen evolution per mol AB versus time plots prepared at various temperatures (Fig. 6a). The activation energy calculated from the slope of the regression line (Fig. 6b) is E_a = 52 ± 2 kJ/mol. The activation energy for the hydrolytic dehydrogenation of ammonia borane catalyzed by Pd(0)/SiO_2–$CoFe_2O_4$

Table 1
Catalytic activity of reported palladium catalysts used for the hydrolytic dehydrogenation of AB.

Entry	Catalyst	TOF (min^{-1})	E_a (kJ/mol)	Ref.
1	$Pd(0)/SiO_2–CoFe_2O_4$	254	52	This study
2	Pd@Co/graphene	37.5	–	[32]
3	$Co_{35}Pd_{65}$/C annealed	35.7	–	[33]
4	2.1 wt% RGO@Pd	26.3	40	[34]
5	$Co_{35}Pd_{65}$/C	22.7	27.5	[33]
6	CDG-Pd	15.5	–	[35]
7	$Pd(0)/SiO_2$	10.0	–	This study
8	Pd(0)-HAP	8.3	55	[36]
9	Pd/zeolite	6.25	56	[37]
10	RGO/Pd	6.25	51	[38]
11	PSSA-*co*-MA-Pd	5	44	[39]
12	$Pd/\gamma\text{-}Al_2O_3$	1.39	–	[40]
13	Pd black	0.67	–	[40]

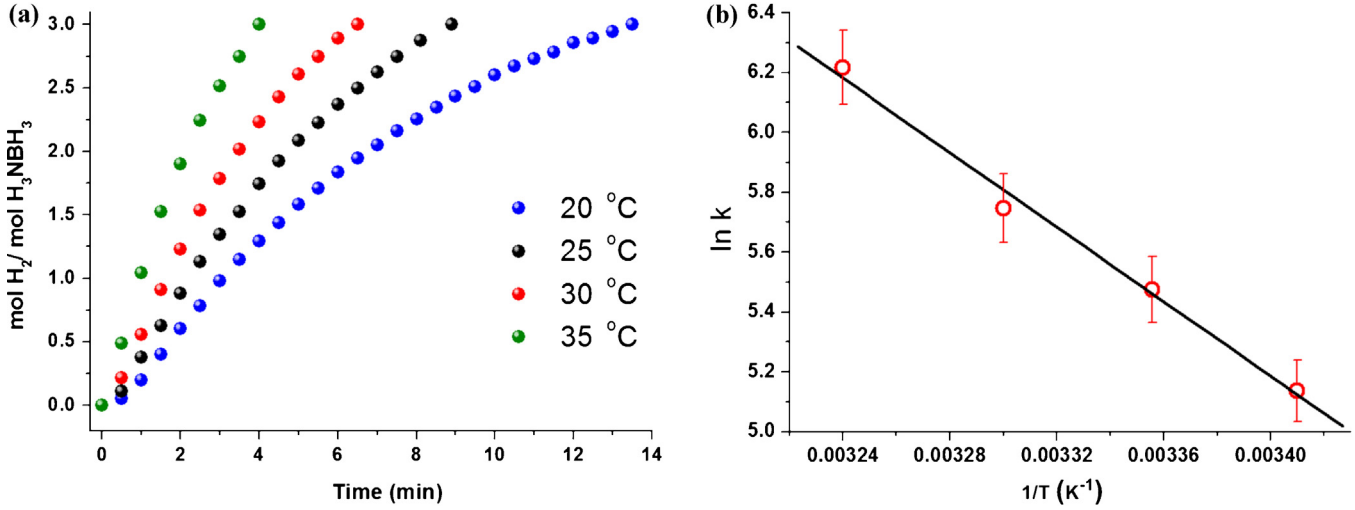

Fig. 6. (a) The evolution of equivalent hydrogen per mole of AB versus time plot for the hydrolytic dehydrogenation of AB starting with $Pd(0)/SiO_2–CoFe_2O_4$ (0.186 mM Pd) and 100 mM AB at various temperatures. (b) The Arrhenius plot for the $Pd(0)/SiO_2–CoFe_2O_4$ catalyzed hydrolytic dehydrogenation of AB. $\ln k = -6225.361(1/T) + 26.35$.

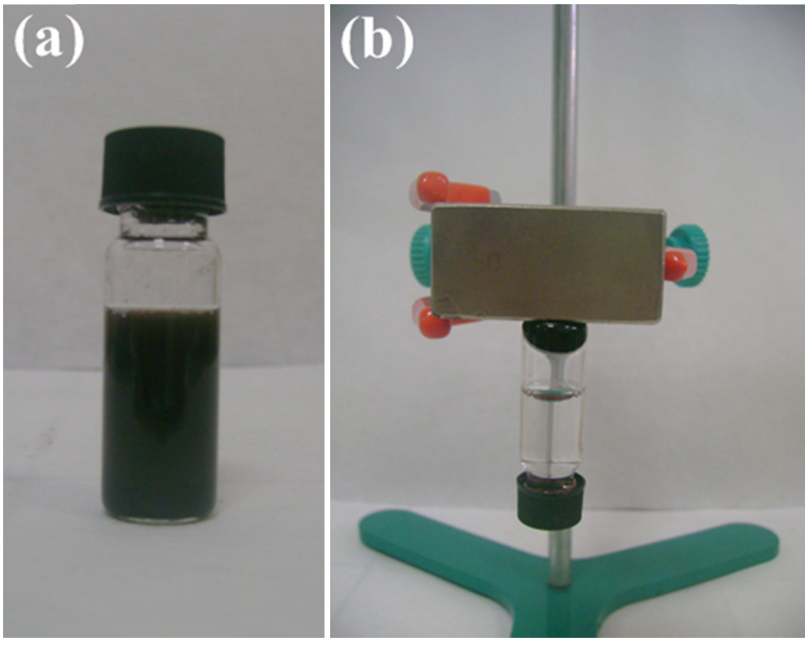

Fig. 7. The pictures of (a) dispersed catalyst in water (b) isolated catalyst using a permanent magnet.

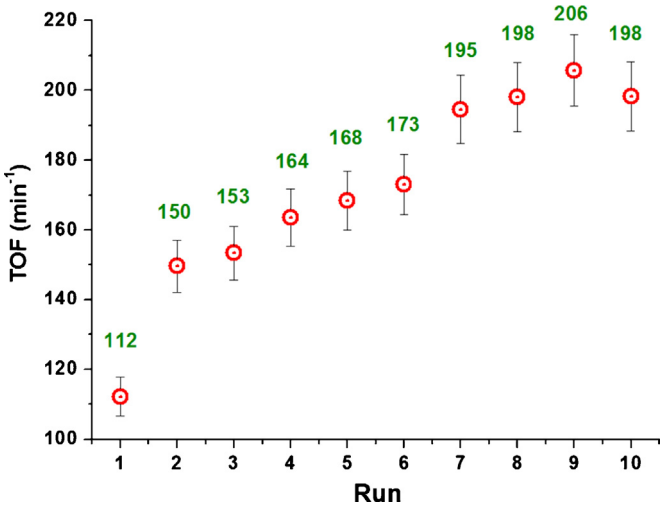

Fig. 8. TOF [mol H_2 (mol Pd min)$^{-1}$] values of Pd(0)/SiO_2–$CoFe_2O_4$ for the subsequent runs.

is comparable with the literature values reported for the other palladium catalysts used in the same reaction (see Table 1).

Reusability of Pd(0)/SiO_2–$CoFe_2O_4$ catalyst was tested in successive experiments performed using the catalyst isolated from the reaction solution after a previous run of hydrolysis of AB. After the completion of hydrogen generation from the hydrolysis of AB starting with 0.744 mM Pd(II)/SiO_2–$CoFe_2O_4$ plus 100 mM AB in 10 mL aqueous solution at 25.0 ± 0.1 °C, the catalyst was isolated using a permanent magnet (Fig. 7b) and washed with 10 mL of water. After washing, the isolated sample of Pd(0)/SiO_2–$CoFe_2O_4$ was redispersed in 10 mL solution containing 100 mM AB and a second run of hydrolysis was started immediately and continued until the completion of hydrogen evolution. Hydrogen generation process was repeated 10 times.

As shown in Fig. 8, the catalytic activity of Pd(0)/SiO_2–$CoFe_2O_4$ increases for the subsequent runs. The increase of TOF values can be attributed to the complete formation of palladium(0) nanoparticles after subsequent runs of hydrolytic dehydrogenation of AB. After each run, the catalyst was isolated using a permanent magnet and the upper solution was separated. The resulting solutions after each subsequent runs were analyzed by ICP-OES and no leaching of Pd into the solution was detected. Therefore, the slight decrease in the catalytic activity of Pd(0)/SiO_2–$CoFe_2O_4$ after 10th run in hydrolytic dehydrogenation of AB can be can be attributed to partial aggregation of nanoparticles on the surface of silica coated cobalt ferrite (see Fig. S3, the TEM image of Pd(0)/SiO_2–$CoFe_2O_4$ after 10th run, in the supporting information). The reusability tests reveal that Pd(0)/SiO_2–$CoFe_2O_4$ are still active in the subsequent runs of hydrolytic dehydrogenation of AB providing 100% conversion, i.e. a release of 3.0 equivalent H_2 per mole of NH_3BH_3 and Pd(0)/SiO_2–$CoFe_2O_4$ still provide the highest TOF value (198 min^{-1}) ever reported catalytic activity even after the 10th use for the hydrolytic dehydrogenation of AB as compared to the palladium catalysts shown in Table 1.

4. Conclusion

In summary, palladium(0) nanoparticles were successfully supported on silica-coated cobalt ferrite and used as catalyst for the hydrolytic dehydrogenation of ammonia borane. Pd(0)/SiO_2–$CoFe_2O_4$ found to be an outstanding catalyst for hydrolytic dehydrogenation of ammonia borane with the highest TOF value among all reported palladium catalysts. They showed remarkably high catalytic activity with an initial turn over frequency of 254 min^{-1} at room temperature. Pd(0)/SiO_2–$CoFe_2O_4$ still provide the highest TOF value (198 min^{-1}) even after the 10th use for the hydrolytic dehydrogenation of ammonia borane as compared to the palladium catalysts. Pd(0)/SiO_2–$CoFe_2O_4$ are highly active, magnetically isolable and recyclable catalysts in hydrogen generation from the hydrolysis of ammonia borane.

Acknowledgments

Partial support of this work by Middle East Technical University, METU Central Laboratory and Turkish Academy of Sciences is gratefully acknowledged.

Appendix A. Supplementary data

Supplementary data associated with this article can be found, in the online version, at http://dx.doi.org/10.1016/j.apcatb.2013.09.023.

References

[1] L. Schlapbach, A. Züttel, Nature 414 (2001) 353–358.
[2] W. Grochala, P.P. Edwards, Chem. Rev. 104 (2004) 1283–1315.
[3] P. Chen, Z. Xiong, J. Luo, J. Lin, K.L. Tan, Nature 420 (2002) 302–304.
[4] N.L. Rosi, J. Eckert, M. Eddaoudi, D.T. Vodak, J. Kim, M.O. Keeffe, O.M. Yaghi, Science 300 (2003) 1127–1129.
[5] A. Staubitz, A.P.M. Robertson, I. Manners, Chem. Rev. 110 (2010) 4079–4124.
[6] P.V. Ramachandran, P.D. Gagare, Inorg. Chem. 46 (2007) 7810–7818.
[7] S. Özkar, S.L. Suib (Eds.), Batteries, Hydrogen Storage and Fuel Cells, Elsevier, Amsterdam, 2013, pp. 165–189.
[8] S. Özkar, R.G. Finke, J. Am. Chem. Soc. 124 (2002) 5796–5810.
[9] S. Özkar, R.G. Finke, Langmuir 18 (2002) 7653–7662.
[10] J.D. Aiken, R.G. Finke, J. Mol. Catal. A: Chem. 145 (1999) 1–44.
[11] G. Wu, X. Wang, N. Guan, L. Li, Appl. Catal., B 136 (2013) 177–185.
[12] A. Barrasa, M.R. Dasb, R.R. Devarapallic, M.V. Shelkec, S. Cordierd, S. Szuneritsa, R. Boukherrouba, Appl. Catal., B 130 (2013) 270–276.
[13] S. Akbayrak, S. Özkar, ACS Appl. Mater. Interfaces 4 (2012) 6302–6310.
[14] X. Yanga, J. Zhenga, M. Zhena, X. Menga, F. Jianga, T. Wanga, C. Shua, L. Jianga, C. Wanga, Appl. Catal., B 121 (2012) 57–64.
[15] H. Liang, G. Chen, S. Desinan, R. Rosei, F. Rosei, D. Ma, Int. J. Hydrogen Energy 3 (2012) 17921–17927.
[16] M. Zahmakıran, S. Akbayrak, T. Kodaira, S. Özkar, Dalton Trans. 39 (2010) 7521–7527.
[17] M. Zahmakıran, S. Özkar, Appl. Catal., B 89 (2009) 104–110.
[18] G.P. Rachiero, U.B. Demirci, P. Miele, Catal. Today 170 (2011) 85–92.
[19] M. Chandra, Q. Xu, J. Power Sources 168 (2007) 135–142.
[20] S. Akbayrak, P. Erdek, S. Özkar, Appl. Catal., B 142–143 (2013) 187–195.
[21] H.J. Chena, H.W. Liua, W. Liaoa, H.B.C. Pana, M. Waia, K.H. Chiud, J.F. Jenb, Appl. Catal., B 111 (2012) 402–408.
[22] J.M. Planeix, N. Coustel, B. Coq, V. Brotons, P.S. Kumbhar, R. Dutartre, P. Geneste, P. Bernier, P.M. Ajayan, J. Am. Chem. Soc. 116 (1994) 7935–7936.
[23] Z.H. Lu, J. Li, A. Zhu, Q. Yao, W. Huang, R. Zhou, R. Zhou, X. Chen, Int. J. Hydrogen Energy 38 (2013) 5330–5337.
[24] K. Maaz, A. Mumtaz, S.K. Hasanain, A. Ceylan, J. Magn. Magn. Mater. 308 (2007) 289–295.
[25] M. Kaya, M. Zahmakıran, S. Özkar, M. Volkan, ACS Appl. Mater. Interfaces 4 (2012) 3866–3873.
[26] W. Stöber, A. Fink, E. Bohn, J. Colloid Interface Sci. 26 (1968) 62–69.
[27] J. Sun, S. Zhou, P. Hou, Y. Yang, J. Weng, X. Li, M. Li, J. Biomed. Mater. Res. Part A 80A (2006) 333–341.
[28] B.L. Cushing, V.L. Kolesnichenko, C.J. O'Connor, Chem. Rev. 104 (2004) 3893–3946.
[29] S. Laurent, D. Forge, M. Port, A. Roch, C. Robic, L. Vander Elst, R.N. Muller, Chem. Rev. 108 (2008) 2064–2110.
[30] Q. Dai, M. Lam, S. Swanson, R-H.R. Yu, D.J. Milliron, T. Topuria, P.-O. Jubert, A. Nelson, Langmuir 26 (2010) 17546–17551.
[31] C.J. Jenks, S.L. Chang, J.W. Anderegg, P.A. Thiel, D.W. Lynch, Phys. Rev. B: Condens. Matter. Mater. Phys. 54 (1996) 6301–6303.
[32] J. Wang, Y.L. Qin, X. Liu, X.B. Zhang, J. Mater. Chem. A: Mater. Energy Sustain 22 (2012) 12468–12470.
[33] D. Sun, V. Mazumder, Ö. Metin, S. Sun, ACS Nano 5 (2011) 6458–6464.
[34] B. Kılıç, S. Şencanlı, Ö. Metin, J. Mol. Catal. A: Chem. 361 (2012) 104–110.
[35] Ö. Metin, E. Kayhan, S. Özkar, J.J. Schneider, Int. J. Hydrogen Energy 37 (2012) 8161–8169.
[36] M. Rakap, S. Özkar, Int. J. Hydrogen Energy 36 (2011) 7019–7027.
[37] M. Rakap, S. Özkar, Int. J. Hydrogen Energy 35 (2010) 1305–1312.
[38] P. Xi, F. Chen, G. Xie, C. Ma, H. Liu, C. Shao, J. Wang, Z. Xu, X. Xu, Z. Zeng, Nanoscale 4 (2012) 5597–5601.
[39] Ö. Metin, Ş. Şahin, S. Özkar, Int. J. Hydrogen Energy 34 (2009) 6304–6313.
[40] Q. Xu, M. Chandra, J. Alloys Compd. 446 (2007) 729–732.